Eur. Phys. J. Special Topics **228**, 2661–2676 (2019)

https://doi.org/10.1140/epjst/e2019-900017-1

THE EUROPEAN PHYSICAL JOURNAL SPECIAL TOPICS

Regular Article

Effects of homogeneous-heterogeneous reactions in flow of nanofluid between two stretchable rotating disks

A. Renuka[1], M. Muthtamilselvan[1,a], Deog-Hee Doh[2], and Gyeong-Rae Cho[2]

[1] Department of Mathematics, Bharathiar University, Coimbatore 641 046, Tamil Nadu, India
[2] Division of Mechanical Engineering, College of Engineering, Korea Maritime and Ocean University, Busan 606 781, South Korea

Received 2 February 2019 / Received in final form 25 March 2019
Published online 6 December 2019

Abstract. The present study analyzes nanofluid flow over a two infinite rotating disk. A magnetic field addressed on momentum equation. An effect of homogeneous-heterogeneous reaction on the fluid flow is investigated. The relevant system of governing equations is transformed into ordinary differential equations by using Von Karman transformations. Homotopy approaches for different physical parameters are examined graphically on appropriate profile. For greater (S_1) the radial, axial and azimuthal velocities are hiked. Energy of liquid enhances with increasing thermophoresis parameter Nt. Local Skin friction coefficient diminishes with higher Reynolds number at lower disk and opposite behavior at upper disk. Moreover concentration field elevates while increasing heterogeneous parameter.

1 Introduction

No doubt the fluid flow through a spinning disk develops at many areas such as oceanography, spinning machinery and so on. Von Karman [1] initially studied about a stretchable spinning disk along with hydrodynamic flow. The prominent transformations are used to convert as a system of nonlinear ODE from nonlinear PDE. Batchelor [2] described one- and two-parameter groups of results of steady rotationally-similar viscous flow. The one-parameter group signifies flow which is rigid-body spinning at infinity and past a plane over the origin. The two-parameter group signifies flow which is rigid body spinning past a two planes at a finite distance apart [2]. Rashidi et al. [3] investigated the hydromagnetic viscous fluid flow through spinning disk with various properties. Few recent research about rotating disk can be mentioned by investigator that were reported in [4–10].

The mixture of nanoparticles that directly colloids with base fluid, such as ethylene glycol, oil or water, is called nanofluid. The advantage of this concept, less volume of string nanoparticles are dispersed in host liquid, and it displays prominent enhancement on thermal conductivity for heat transport activity. Few important nanofluid

[a] e-mail: muthtamil1@buc.edu.in

applications are microelectronics cooling, heating/cooling of home appliances, transportation, cooling towers and so on. Buongiorno [11] studied a two-component four-equation nonhomogeneous equilibrium model for momentum, heat and mass transport using nanofluids about a two four-equation non homogeneous equilibrium model for momentum, heat and mass transport using nanofluids. Hayat et al. [12] studied the MHD nanofluid flow due to a rotating disk with slip effect. Mustafa et al. [13] studied about flow owing to linear infinite disk along with nanoparticles. Hatami et al. [14] examined a laminar incompressible viscous nanoliquid flow caused via spinning disk using LSM. Several researchers discussed various fields in nanofluid [15–19].

Homogeneous and heterogeneous reactions have been extensively analyzed by the recent engineers and scientists. The heterogeneous reaction takes place inside of boundary phase or limited space and the homogeneous reaction frequently increases in the total specified phase. Note that these reactions take place in several procedures like chemical processing, fiber insulation, crops damaging via hydrometallurgical industry, fog formation, freezing and so on. Merkin [20] initially analyzed about chemical reactions effect on flow of boundary layer. He found that the heterogeneous reaction is an influential mechanism neighboring the imperative edge. Chaudhary and Merkin [21] illustrated that a simple model for chemical reactions in stagnation-point boundary-layer flow is made in which the surface reaction by first-order process and the bulk reaction is presumed to be specified through isothermal cubic auto catalator process. Kameswaran et al. [22] studied the chemical reactions impact on flow of nanofluid past a shrinking or stretching sheet located on a porous medium saturated with silver-water and Copper-water nanofluids. Furthermore, modern studies concerning about chemical kinetics are obtained in references [23–29].

We consider the nanofluid flow over a two infinite spinning disks along with chemical reactions and magnetic field. The Chaudhary and Merkin's model [21] has been developed for nanofluids through Buongiorno's nanofluid model [11]. Convergent series solutions are developed through homotopy analysis method. Finally, various kinds of parameter behaviors are examined on suitable field.

2 Formulation of the problem

The three dimensional steady nanofluid flow by two stretchable spinning disks. G_1 and G_2 is angular velocity of lower and upper one. Temperature $T_1 = T_0 + Ar$ and $T_2 = T_0 + Br$ at both disks. Upper one located at $z = h$ ($h = 1$) and lower one placed at $z = 0$ (see Fig. 1). Further a different rate of stretching s_1 and s_2 on both disks. Merkin [20] initiated the fundamental homogenous-heterogeneous reaction model. The homogenous reaction with cubic auto-catalysis defined by [27]

$$C + 2D \to 3D \quad \text{rate} = k_c c d^2 \tag{1}$$

and first order isothermal reaction on the catalysis surface is obtained as [27]

$$C \to D \quad \text{rate} = k_s d. \tag{2}$$

Here both reaction processes are assumed isothermal. The governing equations of this current problem are as follows:

$$\frac{\partial u}{\partial r} + \frac{u}{r} + \frac{\partial w}{\partial z} = 0 \tag{3}$$

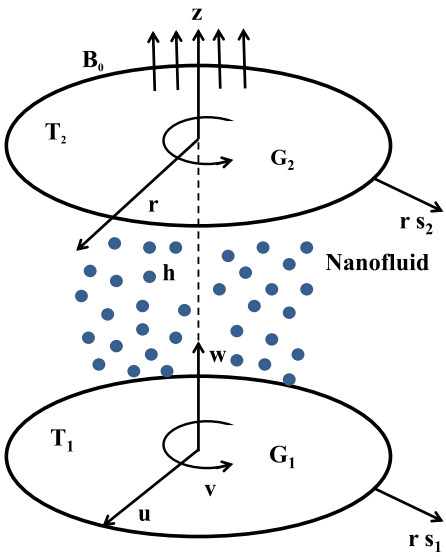

Fig. 1. The flow geometry.

$$u\frac{\partial u}{\partial r}+w\frac{\partial u}{\partial z}-\frac{v^2}{r}=\frac{\partial p}{\partial r}\left(\frac{-1}{\rho}\right)+\nu\left\{\frac{1}{r}\frac{\partial u}{\partial r}+\frac{\partial^2 u}{\partial r^2}-\frac{u}{r^2}+\frac{\partial^2 u}{\partial z^2}\right\}-\frac{\sigma B_0 u}{\rho} \tag{4}$$

$$u\frac{\partial v}{\partial r}+\frac{uv}{r}+w\frac{\partial v}{\partial z}=\nu\left\{\frac{1}{r}\frac{\partial v}{\partial r}+\frac{\partial^2 v}{\partial z^2}-\frac{v}{r^2}+\frac{\partial^2 v}{\partial r^2}\right\}-\frac{\sigma B_0 v}{\rho} \tag{5}$$

$$u\frac{\partial w}{\partial r}+w\frac{\partial w}{\partial z}=\frac{\partial p}{\partial z}\left(\frac{-1}{\rho}\right)+\frac{\partial^2 w}{\partial r^2}+\frac{\partial^2 w}{\partial z^2}+\nu\left\{\frac{1}{r}\frac{\partial w}{\partial r}\right\} \tag{6}$$

$$\rho c_p\left[u\frac{\partial T}{\partial r}+w\frac{\partial T}{\partial z}\right]=k\left\{+\frac{\partial^2 T}{\partial r^2}+\frac{1}{r}\frac{\partial T}{\partial r}+\frac{\partial^2 T}{\partial z^2}\right\}+\tau\left[D_B\left(\frac{\partial T}{\partial z}\frac{\partial C}{\partial z}+\frac{\partial T}{\partial r}\frac{\partial C}{\partial r}\right)+\frac{D_T}{T_2}\left\{\left(\frac{\partial T}{\partial z}\right)^2\right\}+\left(\frac{\partial T}{\partial r}\right)^2\right] \tag{7}$$

$$u\frac{\partial c}{\partial r}+w\frac{\partial c}{\partial z}=D_C\left\{\frac{\partial^2 c}{\partial r^2}+\frac{1}{r}\frac{\partial c}{\partial r}+\frac{\partial^2 c}{\partial z^2}\right\}-k_c c d^2 \tag{8}$$

$$u\frac{\partial d}{\partial r}+w\frac{\partial d}{\partial z}=D_B\left\{\frac{\partial^2 d}{\partial r^2}+\frac{1}{r}\frac{\partial d}{\partial r}+\frac{\partial^2 d}{\partial z^2}\right\}+\frac{D_T}{T_2}\left(\frac{\partial^2 T}{\partial r^2}\right)+\left(\frac{\partial^2 T}{\partial z^2}\right)+k_c c d^2. \tag{9}$$

Appropriate conditions are presented by [27]:

$$v=rG_1,\quad w=0,\quad u=rs_1,\quad T=T_1=T_0+Ar,\quad D_C\frac{\partial c}{\partial z}=k_s c,$$
$$D_B\frac{\partial d}{\partial z}=-k_s c\quad at\ z=0, \tag{10}$$

$$v = rG_2, \quad w = 0, \quad u = rs_2, \quad T = T_2 = T_0 + Br, \quad c \to c_0,$$
$$d \to 0 \quad at\ z = h, \tag{11}$$

where, the velocity components u, v and w is presence of cylindrical coordinates r, θ and z directions. ν is kinematic viscosity, k depicts thermal conductivity, ρ for density, D_B is Brownian diffusion coefficient, T denotes the temperature, c_p is specific heat, D_T indicates thermophoeretic diffusion coefficient, and p denotes the pressure. Here we using Bruggeman model for thermal conductivity. This model shows for binary mixture of homogeneous spherical and randomly dispersed nanoparticle.

$$\mu_{nf} = \frac{\mu_f}{(1-\phi)^{2.5}}, \quad \alpha_{nf} = \frac{k_{nf}}{(\rho c_p)_{nf}},$$
$$(\rho c_p)_{nf} = (1-\phi)(\rho c_p)_{nf} + \phi(\rho c_p)_s, \quad \rho_{nf} = (1-\phi)\rho_f + \phi\rho_s,$$
$$\frac{k_{nf}}{k_f} = \frac{1}{4}\left[(3\phi_s - 1)\frac{k_s}{k_f} + (2 - 3\phi_s) + \sqrt{\Delta}\right] \tag{12}$$
$$\text{where, } \sqrt{\Delta} = (3\phi_s - 1)^2 \left(\frac{k_s}{k_f}\right)^2 + (2 - 3\phi_s)^2 + 2\left(2 + 9\phi_s - 9\phi_s^2\right)\left(\frac{k_s}{k_f}\right).$$

Employing the transformation

$$v = rG_1 g(\zeta), \quad w = -2hG_1 f(\zeta), \quad u = rG_1 f'(\zeta),$$
$$\zeta = \frac{z}{h}, \quad \theta = \frac{T - T_2}{T_1 - T_2}. \tag{13}$$

The continuity equation (1) is automatically satisfied while equations (4)–(9) are converted to

$$\frac{1}{\left(1 - \phi + \phi\frac{\rho_s}{\rho_f}\right)(1-\phi)^{2.5}} f''' + \Lambda + Re\left(g'^{22ff'' - Mf'} - f'^2 +\right) = 0 \tag{14}$$

$$\frac{1}{\left(1 - \phi + \phi\frac{\rho_s}{\rho_f}\right)(1-\phi)^{2.5}} g'' + Re\left(2fg' - 2gf' - Mg\right) = 0, \tag{15}$$

$$4Re\left(1 - \phi + \phi\frac{\rho_s}{\rho_f}\right)(1-\phi)^{2.5} f'f - 2f'' = p', \tag{16}$$

$$\frac{1}{Pr}\frac{k_{nf}/k_f}{\left(1 - \phi + \phi\frac{\rho c_{p_s}}{\rho c_{p_f}}\right)}\theta'' - 2Ref\theta' + Nb\phi'\theta' + N_t\theta'^2 = 0, \tag{17}$$

$$\frac{1}{Sc}\frac{1}{Re}\phi'' + 2f\phi' - k_1\phi l^2 = 0, \tag{18}$$

$$\frac{1}{Sc}\frac{1}{Re}\left(\delta l'' + \frac{Nt}{Nb}\theta''\right) + 2fl' + k_1\phi l^2 = 0, \tag{19}$$

with

$$f^{'}(0)=S_1,\quad p(0)=0,\quad f(0)=0,\quad g(0)=0,\quad \phi^{'}(0)=K_2\phi(0),$$
$$f(1)=0,\quad \delta l^{'}(0)=-K_2\phi(0),\quad g(1)=G,\quad f^{'}(1)=S_2,\quad \theta(1)=0,$$
$$\theta(0)=1,\quad \phi(1)=1,\quad l(1)=0. \tag{20}$$

$$Re=\frac{G_1h^2}{\nu},\quad M=\frac{\sigma B_0^2}{\rho G1},\quad S_1=\frac{s_1}{G_1},\quad S_2=\frac{s_2}{G_1},\quad Nt=\frac{\tau D_T(T_1-T_2)}{T_2\nu},$$
$$Pr=\frac{\rho c_p\nu}{k},\quad G=\frac{G_1}{G_2},\quad k_1=\frac{k_cc_0^2}{G_1},\quad K_2=\frac{k_sh}{D_C},\quad \delta=\frac{D_B}{D_C},\quad Sc=\frac{\nu}{D_C},$$
$$Nb=\frac{\tau c_0D_B}{\nu}. \tag{21}$$

Here M is magnetic parameter, S_1 and S_2 are stretching parameters of lower and upper disks, respectively, Re is Reynolds number, Nt thermophoresis parameter, Pr Prandtl number, k_1 is homogeneous reaction parameter, δ ratio of diffusion coefficient i.e. $\delta=1$, K_2 is heterogeneous reaction parameter, Sc Schmidt number, Nb is Brownian motion parameter. From equation (14) removing the Λ pressure gradient term we obtain

$$\frac{1}{\left(1-\phi+\phi\frac{\rho_s}{\rho_f}\right)(1-\phi)^{2.5}}f^{iv}+Re\left(2ff^{'''}+2gg^{'}-Mf^{''}\right)=0. \tag{22}$$

The diffusion coefficients D_B and D_C are same for two chemical category. We have

$$l(\zeta)+\phi(\zeta)=1. \tag{23}$$

Thus equations (18) and (19) become

$$\frac{1}{Sc}\frac{1}{Re}\left(\phi^{''}+\frac{Nt}{Nb}\theta^{''}\right)-k_1\phi(1-\phi)^2+2f\phi^{'}=0, \tag{24}$$

with

$$\phi(1)=1,\quad \phi^{'}(0)=K_2\phi(0). \tag{25}$$

Shear stresses τ_{zr} and $\tau_{z\theta}$ are given by

$$\tau_{zr}=\mu_{nf}\left.\frac{\partial u}{\partial z}\right|_{z=0}=\frac{\mu_{nf}rG_1}{h}f^{''}(0), \tag{26}$$

$$\tau_{z\theta}=\mu_{nf}\left.\frac{\partial v}{\partial z}\right|_{z=0}=\frac{\mu_{nf}rG_1}{h}g^{'}(0). \tag{27}$$

Entire shear stress τ_{zw} is

$$\tau_{zw}=\sqrt{\tau_{zr}^2+\tau_{z\theta}^2}. \tag{28}$$

Local Skin friction coefficient C_{f2} for upper disk and C_{f1} for lower disk are

$$C_{f2}Re_r^{0.5} = \frac{\left[f^{''}(1)^2 + g^{'}(1)^2\right]^{1/2}}{(1-\phi)^{2.5}}, \tag{29}$$

$$C_{f1}Re_r^{0.5} = \frac{\left[f^{''}(0)^2 + g^{'}(0)^2\right]^{1/2}}{(1-\phi)^{2.5}}, \tag{30}$$

i.e. $Re_r = \frac{rG_1h}{\nu}$.

The rate of heat transport for both disks can be written by

$$Nu_2 = \frac{q_w}{k_f\left(T_1 - T_2\right)}|_{z=h}, \quad Nu_1 = \frac{q_w}{k_f\left(T_1 - T_2\right)}|_{z=0}. \tag{31}$$

Therefore,

$$q_w = -k_{nf}\left(\frac{\partial T}{\partial z}\right)_{z=h}, \quad q_w = -k_{nf}\left(\frac{\partial T}{\partial z}\right)_{z=0}. \tag{32}$$

Thus, the local Nusselt number are attained by

$$Nu_2 = -\frac{k_{nf}}{k_f}\theta^{'}(1), \quad Nu_1 = -\frac{k_{nf}}{k_f}\theta^{'}(0). \tag{33}$$

3 Homotopy procedure

3.1 Zeroth-order deformation problems

The initial values x are

$$f_0\zeta = S_1\zeta - 2S_1\zeta^2 - S_2\zeta^2 + S_1\zeta^3 + S_2\zeta^3, \tag{34}$$

$$g_0\zeta = 1 + (1-G)\,\zeta, \tag{35}$$

$$\theta_0\zeta = -\frac{Nt}{Nb}\zeta, \tag{36}$$

$$\phi_0\zeta = \frac{1}{1+K_2}\,(1 + K_2\zeta). \tag{37}$$

Auxiliary linear operators are

$$\dot{L}_f = f^{'''}, \quad \dot{L}_\theta = \theta^{''}, \quad \dot{L}_g = g^{''}, \quad \dot{L}_\phi = \phi^{''} \tag{38}$$

satisfying the property

$$\dot{L}_f\left[b_1 + b_2\zeta + b_3\zeta^2 + b_4\zeta^3\right] \tag{39}$$

$$\dot{L}_g\left[b_5+b_6\zeta\right] \tag{40}$$

$$\dot{L}_\theta\left[b_7+b_8\zeta\right]=0, \tag{41}$$

$$\dot{L}_\phi\left[b_9+b_{10}\zeta\right]=0, \tag{42}$$

where $b_1, b_2, b_3, ...b_{10}$ are constants.

Non-auxiliary parameters h_f, h_g, h_θ and h_ϕ and embedding parameter $\bar{q}\in[0,1]$ then the zeroth-order deformation problems are

$$(1-\bar{q})\,\dot{L}_f\left[\vec{F}\left(\zeta;\bar{q}\right)-f_0\left(\zeta\right)\right]=h_f\bar{q}N_f\left[\vec{G}\left(\zeta;\bar{q}\right),\vec{F}\left(\zeta;\bar{q}\right)\right], \tag{43}$$

$$(1-\bar{q})\,\dot{L}_g\left[\vec{G}\left(\zeta;\bar{q}\right)-g_0\left(\zeta\right)\right]=h_g\bar{q}N_g\left[\vec{F}\left(\zeta;\bar{q}\right),\vec{G}\left(\zeta;\bar{q}\right)\right], \tag{44}$$

$$(1-\bar{q})\,\dot{L}_\theta\left[\hat{\theta}\left(\zeta;\bar{q}\right)-\theta_0\left(\zeta\right)\right]=h_\theta\bar{q}N_\theta\left[\vec{F}\left(\zeta;\bar{q}\right),\vec{\theta}\left(\zeta;\bar{q}\right),\vec{\phi}\left(\zeta;\bar{q}\right)\right], \tag{45}$$

$$(1-\bar{q})\,\dot{L}_\phi\left[\hat{\phi}\left(\zeta;\bar{q}\right)-\phi_0\left(\zeta\right)\right]=h_\phi\bar{q}N_\phi\left[\vec{\theta}\left(\zeta;\bar{q}\right),\vec{\phi}\left(\zeta;\bar{q}\right),\vec{F}\left(\zeta;\bar{q}\right)\right], \tag{46}$$

$$\vec{F}'\left(1;\bar{q}\right)=S_2,\quad \vec{F}\left(1;\bar{q}\right)=0,\quad \vec{F}\left(0;\bar{q}\right)=0,\quad \vec{F}'\left(0;\bar{q}\right)=S_1, \tag{47}$$

$$\vec{G}\left(1;\bar{q}\right)=G,\quad \vec{G}\left(0;\bar{q}\right)=1, \tag{48}$$

$$\vec{\theta}\left(1;\bar{q}\right)=0,\quad \vec{\theta}\left(0;\bar{q}\right)=1, \tag{49}$$

$$\vec{\phi}\left(1;\bar{q}\right)=1,\quad \vec{\phi}'\left(0;\bar{q}\right)=K_2\vec{\phi}. \tag{50}$$

Non-linear differential operatives N_f, N_g, and N_θ are

$$N_f\left[\vec{G}\left(\zeta;\bar{q}\right),\vec{F}\left(\zeta;\bar{q}\right)\right]=\left(\frac{1}{\left(1-\phi+\frac{\phi\rho_s}{\phi\rho_f}\right)\left(1-\phi\right)^{2.5}}\right)\frac{\partial^4\vec{F}\left(\zeta;\bar{q}\right)}{\partial\zeta^4}-ReM\frac{\partial^2\vec{F}\left(\zeta;\bar{q}\right)}{\partial\zeta^2}$$
$$+\;2Re\vec{F}\left(\zeta;\bar{q}\right)\frac{\partial^3\vec{F}\left(\zeta;\bar{q}\right)}{\partial\zeta^3}+2Re\vec{G}\left(\zeta;\bar{q}\right)\frac{\partial\vec{G}\left(\zeta;\bar{q}\right)}{\partial\zeta} \tag{51}$$

$$N_g\left[\vec{G}\left(\zeta;\bar{q}\right),\vec{F}\left(\zeta;\bar{q}\right)\right]=\left(\frac{1}{\left(1-\phi+\frac{\phi\rho_s}{\phi\rho_f}\right)\left(1-\phi\right)^{2.5}}\right)\frac{\partial^2\vec{G}\left(\zeta;\bar{q}\right)}{\partial\zeta^2}-ReM\vec{G}\left(\zeta;\bar{q}\right)$$
$$+\;2Re\vec{F}\left(\zeta;\bar{q}\right)\frac{\partial\vec{G}\left(\zeta;\bar{q}\right)}{\partial\zeta}-2Re\frac{\partial\vec{F}\left(\zeta;\bar{q}\right)}{\partial\zeta}\vec{G}\left(\zeta;\bar{q}\right) \tag{52}$$

$$N_\theta\left[\vec{\theta}\left(\zeta;\bar{q}\right),\vec{G}\left(\zeta;\bar{q}\right)\right]=\left(\frac{k_{nf}}{k_f}\right)\left(1-\phi+\frac{\phi\rho c_{p_s}}{\phi\rho c_{p_f}}\right)\frac{\partial^2\vec{\theta}\left(\zeta;\bar{q}\right)}{\partial\zeta^2}-Nt\left(\frac{\partial\vec{\theta}\left(\zeta;\bar{q}\right)}{\partial\zeta}\right)^2$$
$$+\;2Re\vec{F}\left(\zeta;\bar{q}\right)\frac{\partial\vec{\theta}\left(\zeta;\bar{q}\right)}{\partial\zeta}+Nb\frac{\partial\vec{\theta}\left(\zeta;\bar{q}\right)}{\partial\zeta}\frac{\partial\vec{\phi}\left(\zeta;\bar{q}\right)}{\partial\zeta} \tag{53}$$

$$N_\phi\left[\vec{\theta}\left(\zeta;\bar{q}\right),\vec{G}\left(\zeta;\bar{q}\right)\right]=\frac{1}{Re}\frac{1}{Sc}\left(\frac{\partial^2\vec{\phi}\left(\zeta;\bar{q}\right)}{\partial\zeta^2}+\frac{Nt}{Nb}\frac{\partial^2\vec{\theta}\left(\zeta;\bar{q}\right)}{\partial\zeta^2}\right)$$
$$+\,2\vec{F}\frac{\partial\vec{\phi}\left(\zeta;\bar{q}\right)}{\partial\zeta}-\,k_1\vec{\phi}\left(1-\vec{\phi}\right)^2. \tag{54}$$

3.2 *m*th order deformation problem

The mth order deformation problems are

$$L_f\left[f_m(\zeta)-\tilde{\chi_m}f_{m-1}(\zeta)\right]=h_f R_{f,m}(\zeta), \tag{55}$$

$$L_g\left[g_m(\zeta)-\tilde{\chi_m}g_{m-1}(\zeta)\right]=h_g R_{g,m}(\zeta), \tag{56}$$

$$L_\theta\left[\theta_m(\zeta)-\tilde{\chi_m}\theta_{m-1}(\zeta)\right]=h_\theta R_{\theta,m}(\zeta), \tag{57}$$

$$L_\phi\left[\phi_m(\zeta)-\tilde{\chi_m}\phi_{m-1}(\zeta)\right]=h_\phi R_{\phi,m}(\zeta), \tag{58}$$

where $R_{f,m}(\zeta)$, $R_{g,m}(\zeta)$ and $R_{\theta,m}(\zeta)$ are

$$\begin{aligned}R_{f,m}(\zeta)=&\left(\frac{1}{(1-\phi)^{2.5}\left(1-\phi+\frac{\phi\rho_s}{\phi\rho_f}\right)}\right)f_{m-1}^{iv}-Re\left(Mf_{m-1}^{''}\right.\\&\left.-2\sum_{k=0}^{m-1}\left(f_{m-1-k}f_k^{'''}+g_{m-1-k}g_k^{'}\right)\right),\end{aligned} \tag{59}$$

$$\begin{aligned}R_{g,m}(\zeta)=&\left(\frac{1}{(1-\phi)^{2.5}\left(1-\phi+\frac{\phi\rho_s}{\phi\rho_f}\right)}\right)g_{m-1}^{''}+Re\left(+Mg_{m-1}\right.\\&\left.-2\sum_{k=0}^{m-1}\left(f_{m-1-k}g_k^{'}-f_{m-1-k}^{'}g_k\right)\right),\end{aligned} \tag{60}$$

$$\begin{aligned}R_{\theta,m}(\zeta)=&\left(\frac{k_{nf}}{k_f}\right)\left(1-\phi+\frac{\phi\rho c_{p_s}}{\phi\rho c_{p_f}}\right)\theta_{m-1}^{''}+Re2\sum_{k=0}^{m-1}\left(f_{m-1-k}\theta_k^{'}\right)\\&+Nb\sum_{k=0}^{m-1}\theta_{m-1-k}^{'}\phi_k^{'}+Nt\sum_{k=0}^{m-1}\theta_{m-1-k}^{'}\theta_k^{'}\end{aligned} \tag{61}$$

$$\begin{aligned}R_{\phi,m}(\zeta)=&\frac{1}{Re}\frac{1}{Sc}\left(\phi_{m-1}^{''}+\frac{Nt}{Nb}\phi_{m-1}^{''}\right)+2\sum_{k=0}^{m-1}\left(f_{m-1-k}\phi_k^{'}\right)\\&-k_1\phi_{m-1}\left(1-\phi_{m-1}\right)^2\end{aligned} \tag{62}$$

$$\chi_m^{\check{}}=\begin{cases}0, & m\le 1,\\ 1, & m>1.\end{cases} \tag{63}$$

The mth term in following manner

$$f_m(\zeta)=\vec{F_m}(\zeta)+b_1+c_2\zeta+b_3\zeta^2+b_4\zeta^3, \tag{64}$$

$$g_m(\zeta)=\vec{G_m}(\zeta)+b_5+b_6\zeta, \tag{65}$$

$$\theta_m(\zeta)=\vec{\Theta_m}(\zeta)+b_7+b_8\zeta, \tag{66}$$

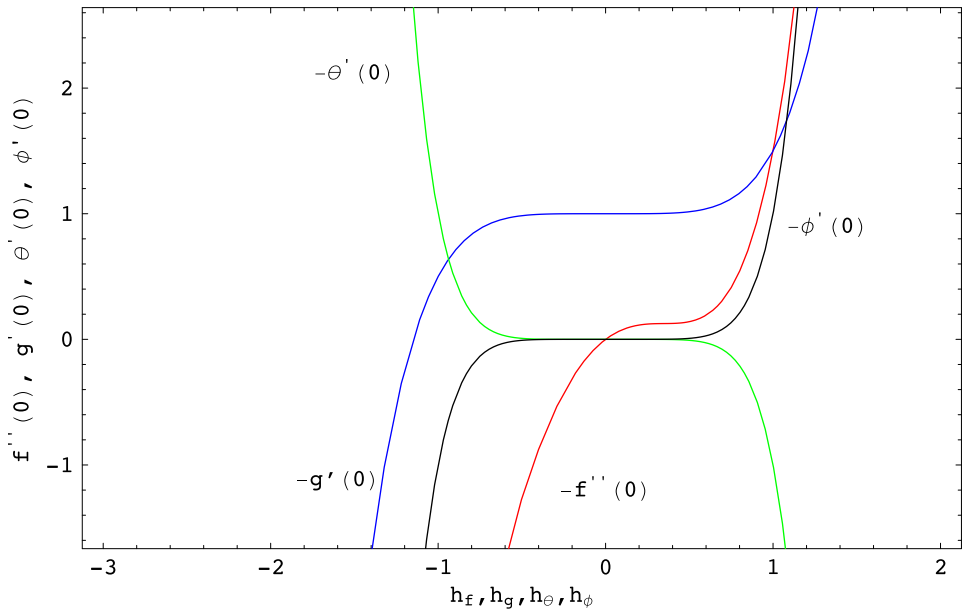

Fig. 2. h-curves for $-f''(0), -g'(0), -\theta'(0)$ and $-\phi'(0)$.

$$\phi_m(\zeta) = \vec{\phi_m}(\zeta) + b_9 + b_{10}\zeta, \tag{67}$$

i.e. particular solutions are $\hat{F_m}(\zeta), \hat{G_m}(\zeta), \hat{\Theta_m}(\zeta)$ and $\hat{\Phi_m}(\zeta)$.

4 Result and discussion

This paper analyzes the homogeneous-heterogeneous reaction and magnetic field in nanofluid flow among dual stretchable spinning disks. Effect of different parameters are magnetic field M, Reynolds number Re, lower stretching parameter S_1, upper stretching parameter S_2, Prandtl number Pr, rotation parameter G, thermophoresis parameter Nt, chemical reaction parameter k_1 and K_2 and Brownian motion parameter Nb on the velocity (axial, radial and azimuthal), concentration, temperature and local skin friction coefficient are scrutinized through graphical manner.

Homotopy contains an embedding auxiliary parameter h which provides the independence to choose and adjust convergence core of series solutions. The h-curves are plotted to get effective ranges of these parameters (see Fig. 2). We have drawn h-curves at 20th-order approximations to acquire ranges of these parameter. The permissible values of h_f, h_g, h_θ, and h_ϕ are $0.2 \leq h_f \leq 0.4$, $-0.4 \leq h_g \leq 0.4$, $-0.4 \leq h_\theta \leq 0.4$, and $-0.4 \leq h_\phi \leq 0.4$, respectively. Figures 3 and 4 depict the behavior of magnetic field M on the azimuthal $g(\zeta)$ and axial $f(\zeta)$ velocity profile. While we increase M, both azimuthal $g(\zeta)$ and axial $f(\zeta)$velocity profiles decrease. Because Lorentz force and magnetic field are connected with each other when it is applied to the fluid, it reduces the motion of the fluid particles. Figure 5 presents the Reynolds number Re impact on the $g(\zeta)$. Here azimuthal velocity $g(\zeta)$ reduces when Re is increased. The ratio between inertial force and viscous force is called Reynolds number. Therefore, velocity reduces for higher Reynolds number because of very less force of viscous. Figures 6–8 demonstrates the stretching parameter S_1

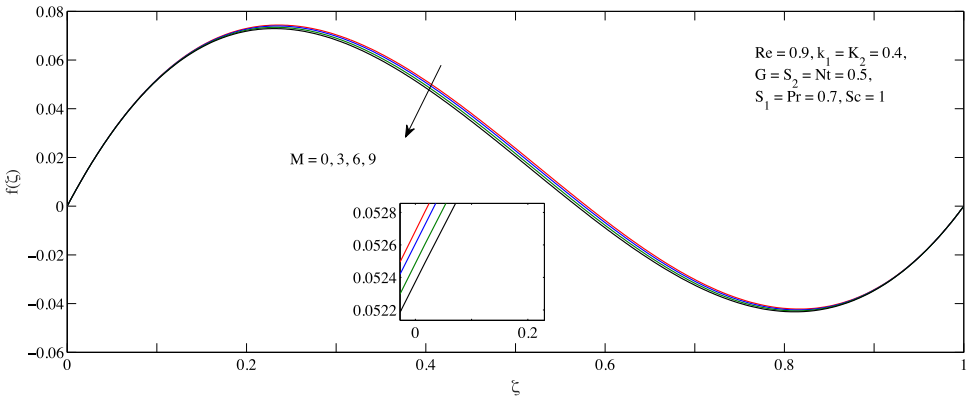

Fig. 3. Effect of M on f(ζ).

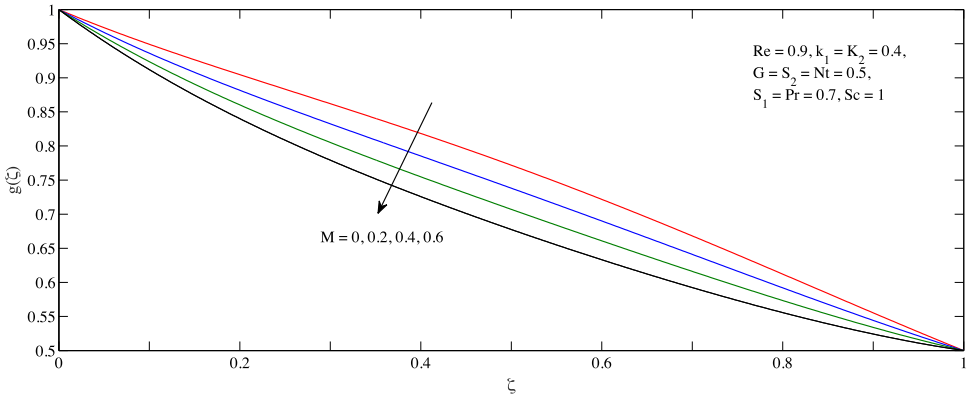

Fig. 4. Effect of M on g(ζ).

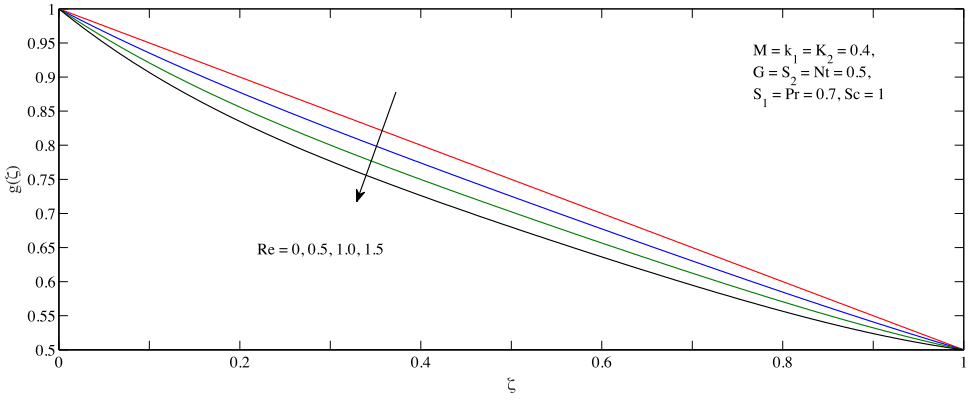

Fig. 5. Effect of Re on g(ζ).

effect on velocity of radial, axial and azimuthal profile. Here we found that the magnitude of axial velocity $f(\zeta)$ increases at lower one meanwhile an opposite behavior is noted at above one. However, axial and radial velocity profiles take negative values at upper disk by elevating S_1 in Figures 6 and 7. Moreover, the volume of azimuthal

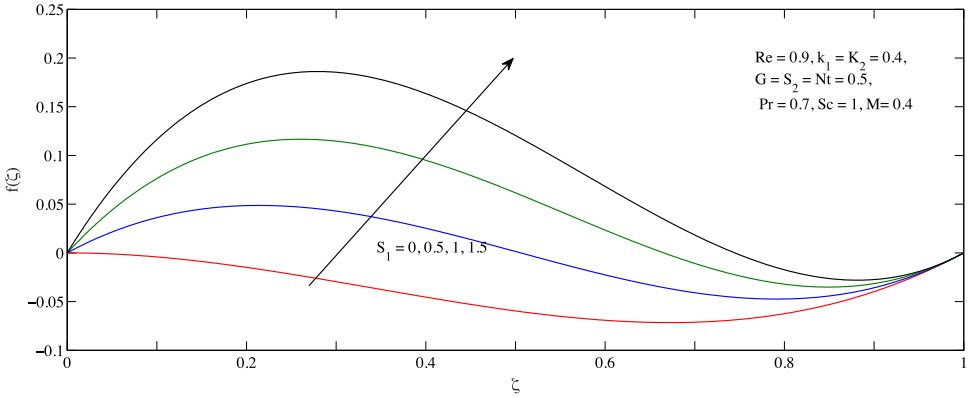

Fig. 6. Effect of S_1 on f(ζ).

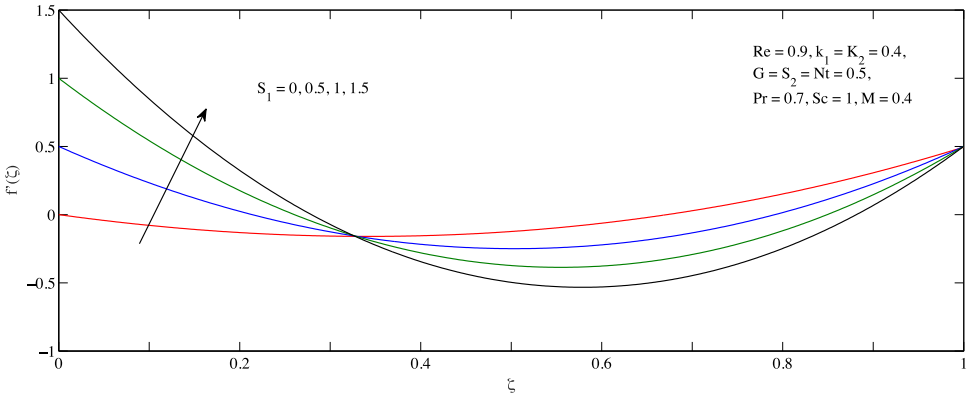

Fig. 7. Effect of S_1 on f'(ζ).

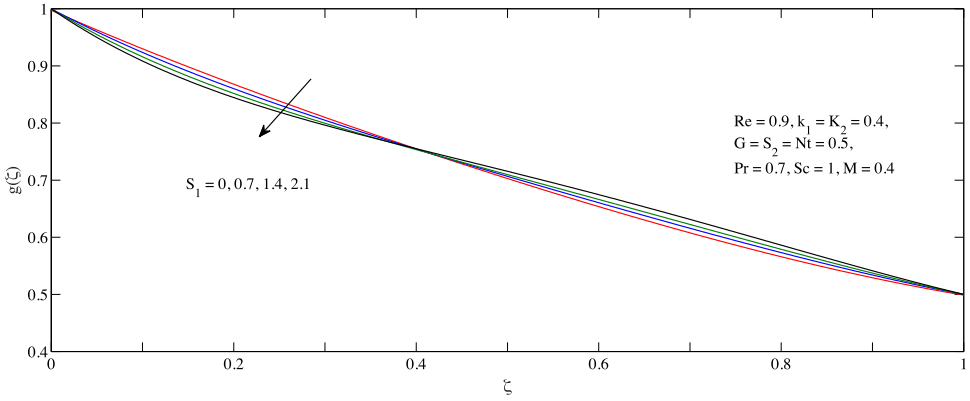

Fig. 8. Effect of S_1 on g(ζ).

velocity $g(\zeta)$ decreases when we increase the value of lower stretching parameter S_1 in Figure 8.

The influence of upper stretching parameter S_2 on radial velocity profile is depicted in Figure 9. Magnitude of radial $f'(\zeta)$ velocity enhances near upper one

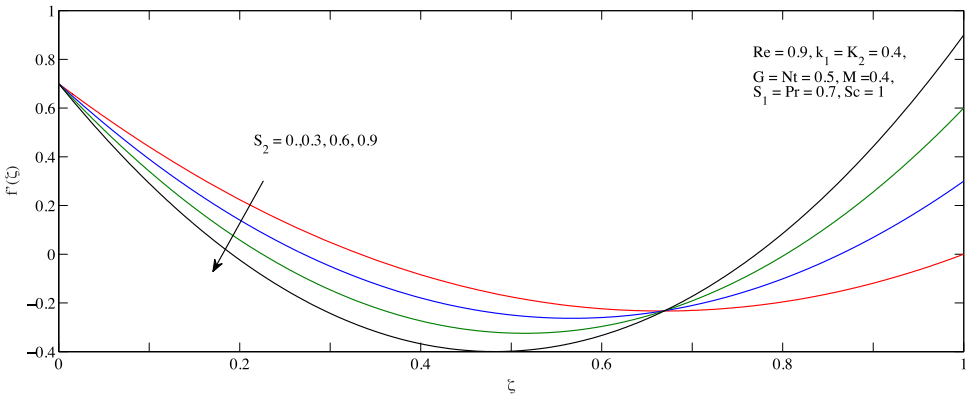

Fig. 9. Effect of S_2 on f'(ζ).

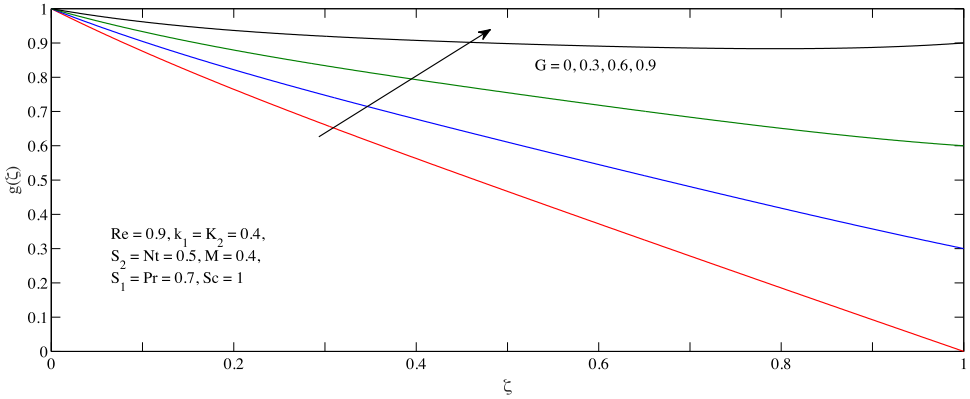

Fig. 10. Effect of G on g(ζ).

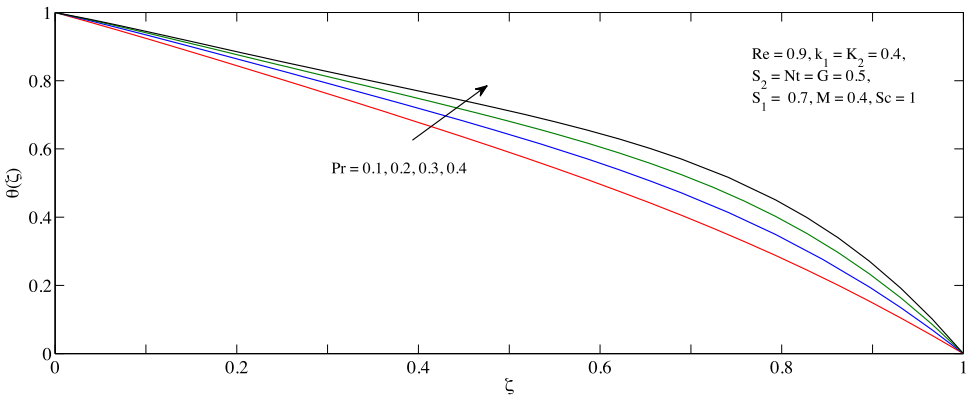

Fig. 11. Effect of Pr on $\theta(\zeta)$.

and also declines near lower one with higher S_2. Moreover, reverse behavior was noticed at an opposite disk. Rotational parameter G effect on azimuthal velocity $g(\zeta)$ profile is shown in Figure 10. Here $g(\zeta)$ elevates with higher rotation parameter G. The following figures of temperature profiles are plotted and demonstrated for the various values of Nt, Pr and Nb of nanofluid. Figure 11 elucidates the behavior of

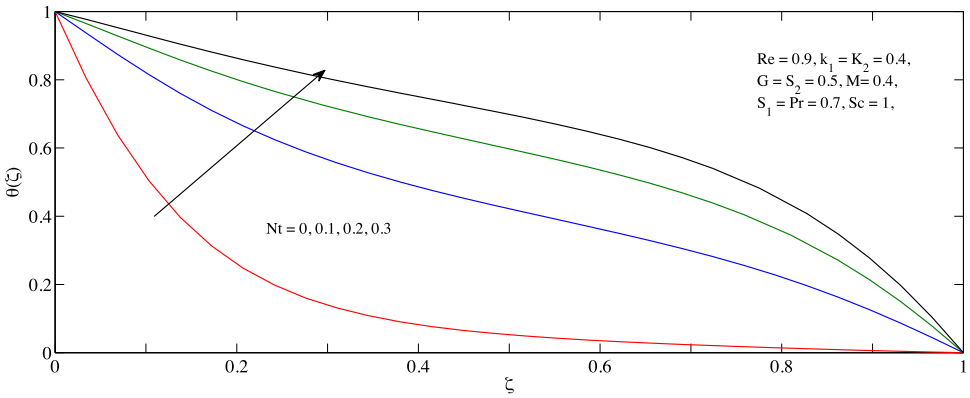

Fig. 12. Effect of Nt on $\theta(\zeta)$.

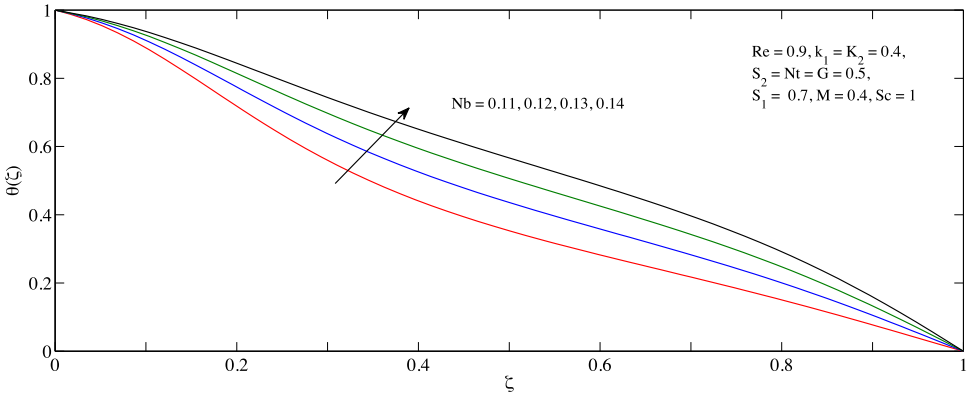

Fig. 13. Effect of Nb on $\theta(\zeta)$.

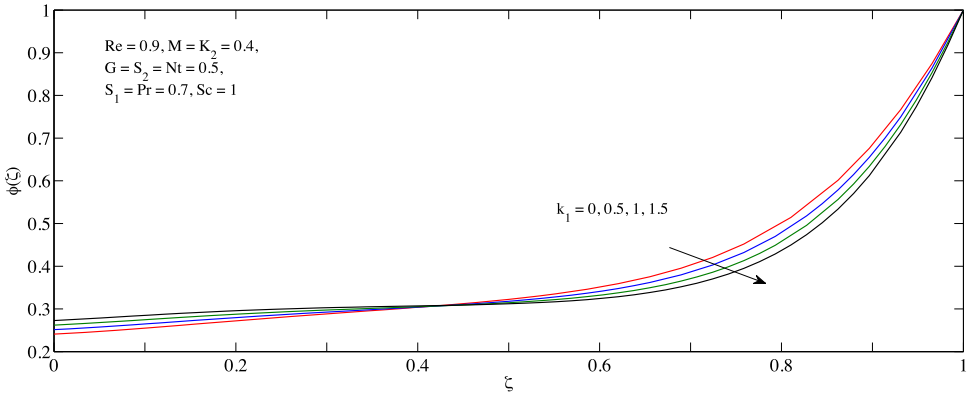

Fig. 14. Effect of k_1 on $\phi(\zeta)$.

Prandtl number Pr on temperature profile. A ratio of momentum and thermal diffusivity is called Prandtl number. Here an increase in Prandtl number Pr indicates stronger momentum diffusivity which is the real reason toward raising the temperature structure [15]. The behavior of thermophoresis parameter Nt on the temperature profile $\theta(\zeta)$ is sketched in Figure 12. Thermophoresis parameter is enhanced due to

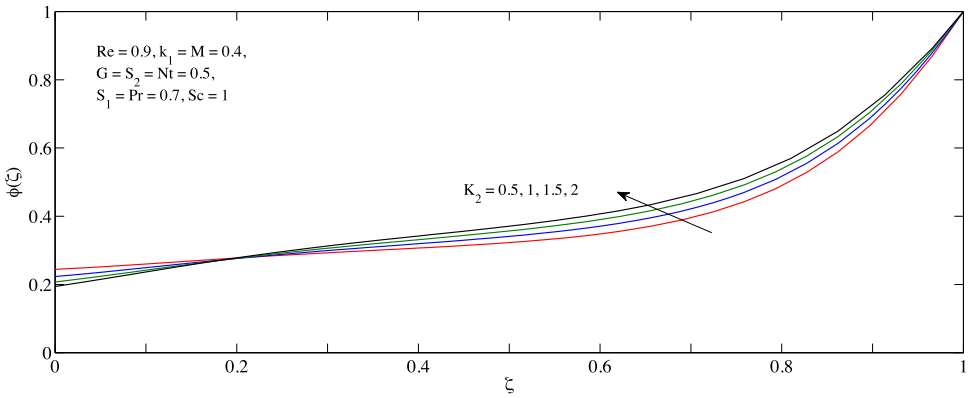

Fig. 15. Effect of K_2 on $\phi(\zeta)$.

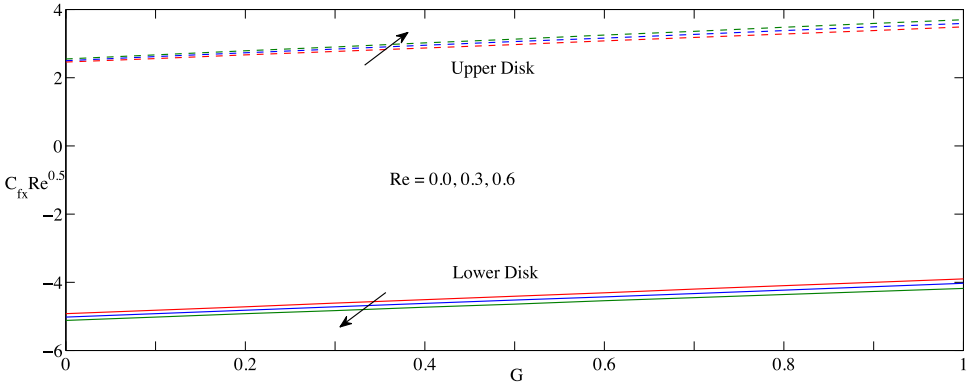

Fig. 16. Effect of Re on $C_{fx}Re^{0.5}$.

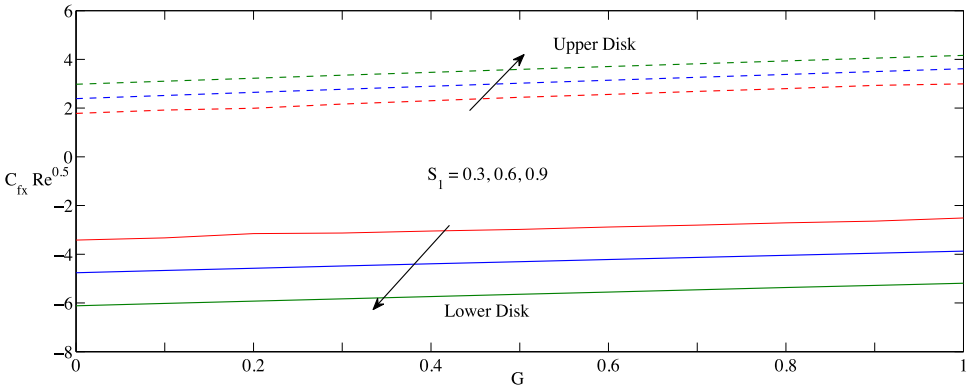

Fig. 17. Effect of S_1 on $C_{fx}Re^{0.5}$.

temperature of the fluid increase. Physical thermophoretic force enhances for larger Nt because the nanoparticles can migrate from warm region to cool region and also enhances the liquid temperature. Figure 13 illustrates the impact of Brownian motion parameter Nb on $\theta(\zeta)$; temperature augments for larger Nb. While hiking Nb gives

Table 1. Heat transfer rate at the lower and upper disks for different physical parameters.

Pr	Nb	Re	Nt	Nu_1	Nu_2
0.1	0.5	0.9	0.5	1.6939	4.0298
0.2				1.3583	5.3176
0.3				1.1640	6.5253
0.7	0.1			1.9958	1.1252
	0.15			0.9658	4.9500
	0.17			0.8134	6.4194
		0.1		0.6145	6.9015
		0.3		0.6643	7.8384
		0.5		0.7133	8.8540
			0.3	1.6247	7.9048
			0.4	1.1220	9.6561
			0.5	0.8084	11.0919

greater arbitrary move of particles, which reasons toward enhance structure of energy and also boundary layer thickness [15].

Figures 14 and 15 plotted the effects of homogeneous k_1 and heterogeneous K_2 reaction parameter on the concentration profile. Figures 14 and 15 elucidated the homogeneous and heterogeneous reaction impact on $\phi(\zeta)$ for nanofluid. Here the concentration profiles decreases for greater k_1 and elevates for different values of K_2. Figures 16 and 17 presented Re, lower stretching parameter S_1 and G upon skin friction of lower and upper disks. The surface drag force decreases for various Re at lower disk when reverse things depict at above one (see Fig. 16). Similarly, Figure 17 shows the effect of stretching parameter S_1 on skin friction coefficient. It is noted for larger S_1 the surface drag force augments at above disk and decreases at below disk. Table 1 shows the impact of involved parameters on Nusselt number. Rate of heat transport enhances for higher Pr, Nb and Nt at upper disk while at lower disk it depicts decreasing behavior. For larger Reynolds number the heat transfer rate enhances at both lower and upper disks.

5 Conclusion

In this study, we have considered the characteristics of homogeneous-heterogeneous reaction on boundary layer flow of nanofluid flow between two parallel rotating disks with magnetic field analyzed. Buongiorno's nanofluid model [11] was utilized under the governing equations. Thus, we explained some exciting effect of pertinent parameters associated with governing equations. Our important findings are concluded as follows:

- Azimuthal velocity hikes and both velocity of axial and radial decays on upper one with greater S_2.
- Opposite behavior of rotational parameter is noted for axial and azimuthal velocity profile.
- Temperature profile increases for both thermophoresis parameter and Prandtl number.
- Fluid concentration decays with large values of k_1, Re and S_1 while increases for S_2.

– For greater Reynolds number, opposite effect is observed on surface drag force at both disks.

This research was supported by Basic Science Research Program through the National Research Foundation of Korea (NRF) funded by the Korea Government (No.2017R1A2B2010603) and (2018R1A2B6009387). This has been also supported by the Program of Business Cooperative R&D (R0006261) funded by MOTIE.

References

1. T. Von Karman, Z. Angew. Math. Mech. **1**, 233 (1921)
2. G.K. Batchelor, Q. J. Mech. Appl. Math. **4**, 29 (1951)
3. M.M Rashidi, N. Kavyani, S. Abelman, Int. J. Heat Mass Transfer **70**, 892 (2014)
4. M.M. Rahman, A. Postelnicu, Mech. Res. Commun. **37**, 598 (2010)
5. U.T. Bodewadt, Z. Angew Math. Mech. **20**, 241 (1940)
6. M. Turkyilmazoglu, AIP Phys. Fluids **28**, 1070 (2016)
7. M. Imtiaz, T. Hayat, A. Alsaedi, S. Asghar, Results Phys. **7**, 503 (2017)
8. T. Hayat, S. Qayyum, M. Imtiaz, A. Alsaedi, Results Phys. **7**, 126 (2017)
9. N. Bachok, A. Ishak, I. Pop, Physica B **406**, 1767 (2011)
10. M. Mustafa, Int. J. Heat Mass Transfer **108**, 1910 (2017)
11. J. Buongiorno, J. Heat Transfer **128**, 240 (2006)
12. T. Hayat, T. Muhammada, S.A Shehzadc, A. Alsaedi, Comput. Methods Appl. Mech. Eng. **315**, 467 (2017)
13. M. Mustafa, J.A. Khan, T. Hayat, A. Alsaedi, J. Mol. Liq. **211**, 119 (2015)
14. M. Hatami, M. Sheikholeslami, D.D. Ganji, Powder Technol. **253**, 769 (2014)
15. T. Hayat, M. Javed, M. Imtiaz, A. Alsaedi, J. Mol. Liq. **240**, 291 (2017)
16. R. Ul Haq, N.F.M. Noor, Z.H. Khan, Adv. Powder Technol. **27**, 1568 (2016)
17. T. Hayat, T. Muhammad, S.A. Shehzad, G.Q. Chen, I.A. Abbas, J. Magn. Magn. Mater. **389**, 48 (2015)
18. T. Hayat, M. Imtiaz, A. Alsaedi, M.A. Kutbi, J. Magn. Magn. Mater. **396**, 31 (2015)
19. M. Mustafa, J.A. Khan, T. Hayat, A. Alsaedi, J. Mol. Liq. **211**, 119 (2015)
20. J.H. Merkin, Math. Comput. Modell. **24**, 125 (1996)
21. M.A. Chaudhary, J.H. Merkin, Fluid Dyn. Res. **16**, 311 (1995)
22. P.K. Kameswaran, S. Shaw, P. Sibanda, P.V.S.N. Murthy, Int. J. Heat Mass Transfer **57**, 465 (2013)
23. T. Hayat, Z. Hussain, A. Alsaedi, Results Phys. **6**, 1161 (2016)
24. T. Yasmeen, T. Hayat, M.I. Khan, M. Imtiaz, A. Alsaedi, J. Mol. Liq. **223**, 1000 (2016)
25. I.L. Animasaun, C.S.K. Raju, N. Sandeep, Alexandria Eng. J. **55**, 1595 (2016)
26. P.V.S. Narayana, D.H. Babu, J. Taiwan Inst. Chem. Eng. **59**, 18 (2016)
27. T. Hayat, S. Qayyum, M. Imtiaz, A. Alsaedi, Results Phys. **7**, 2557 (2017)
28. M. Muthtamilselvan, A. Renuka, Multidiscipline Model. Mater. Struct. **5**, 1115 (2018)
29. M. Muthtamilselvan, A. Renuka, D.H. Doh, J. Nanofluids. **8**, 1496 (2019)